3rd International Structural Specialty Conference
3ième conférence internationale spécialisée sur le génie des structures

Edmonton, Alberta
June 6-9, 2012 / *6 au 9 juin 2012*

Long-term Performance of Reinforced Concrete Beams with GFRP Bars After Accelerated Aging

Yeonho Park[1], Guillermo Ramirez[2], Ali Abolmaali[1]
[1] Department of Civil Engineering, University of Texas at Arlington
[2] Exponent® Failure Analysis Associates

Abstract: The use of fiber-reinforced polymer (FRP) bars in reinforced concrete (RC) structures has emerged as an alternative to traditional steel reinforcement environments and other applications where steel has shown greater vulnerability. Although the number of analytical and experimental studies on RC beams with FRP reinforcement has increased in recent decades, its long term performance is still questioned in comparison to the traditional steel reinforcement. This study presents the results and discussion of an experimental study concerning long-term behaviors of concrete beams reinforced with glass-FRP (GFRP) bars after accelerated aging in an environmental chamber at 115˚F(80% of relative humidity) up to 300 days. Two types (Wrapped surface / Sand-coated surface) of GFRP bars were used. All beams were clamped in pairs using transverse steel rods at the beam end to simulate cracks typical of those produced by in service conditions. Prior to exposure in the chamber, beams were precracked to levels representative to those seen during service loads. In all cases, however, the moment carrying capacity decreased and the deflection increased as a function of time when exposing in circumstances for accelerated aging. The change of load-carrying capacity in RC-steel specimens is greater than the one in RC-GFRP specimens. Comparison of deformability factor for compression failures of RC-GFRP beams and RC-steel beams indicates that the values are not similar before and after exposing into accelerated aging.

1. Introduction

According to the ASCE infrastructure report (Report card for America's infrastructure,2009), 27 percents of the inspected national bridges were classified as defective structurally or functionally due to corrosion of steel reinforcement bars. Numerous reinforced concrete structures are unlikely to reach their expected service life as the result from long term exposure to aggressive environments such as severe weather and de-icing salts that result in corrosion. To reduce corrosion problem of steel reinforcement, this drawback of corrosion led many researches to the development of non-metallic materials such as Fiber Reinforced Polymer (FRP) for reinforcement. Research programs carried out during the last two decades have demonstrated that FRP is the one of the potential solutions to solve the problem regarding corrosion in reinforced concrete structures by using them as a replacement for traditional steel reinforcement. The development of reinforced concrete with Glass Fiber Reinforced Polymer (GFRP) bars and their application in civil infrastructures is getting a great deal of interests from civil engineering field (El-Salakawy et al, 2003). However, determination of long-term performance is a recognized but less-mentioned topic in the field of reinforced concrete with FRP bars. It is a need to validate long-term performance of FRP reinforced concrete structures, and accelerated testing can provide the data for this validation. In order to predict long-term behavior of reinforced concrete with GFRP bars (RC-GFRP), it is critical to determine the effects that long term exposure to the environment can have in degrading the composite materials.

Research in a number of FRP bars, including Glass, Aramid and Carbon fiber, have been extensively conducted to investigate the strength, serviceability and long-term behaviors of the bars alone (Benmokrane et al,1996). Analytical and experimental studies for environmental durability of the FRP material itself for civil infrastructures were reported (Karbhari et al, 2002 and 2003). The results of these studies showed not only the relationship between degradation and matrix/fibers interface but also the effects of moisture and alkalis on GFRP bars. That is, these studies demonstrated that the durability of the composites is affected by increase of water temperature and water absorption under the influence of combined moisture and temperature for a short duration. Moreover, the authors also suggested coefficient of reduction dropping strength of the composite materials after short and long terms of exposure.

A correlation formula between accelerated weathering in the laboratory and natural weathering in the field was proposed (Vijay et al, 1999). An accelerated aging methodology predicted the degradation in the mechanical properties of FRP under the given duration and its relationship with the natural aging. Nevertheless, this project was not conducted for FRP reinforcing bars embedded in concrete under sustained stress level but for FRP bars not embedded in concrete with stress and for FRP bars embedded in concrete without stress, this condition did not present a realistic representation of a real world exposure profile. This did not result in an accurate representation of the degradation on concrete structures reinforced with GFRP bars. Moreover, studies conducted in United Kingdom showed that the long-term strength of glass fiber reinforced cement (GRC) in any climate can be predicted by using accelerated aging methodology (Litherland et al, 1981). This proposed method demonstrated the validity of using accelerated tests with real natural aging of composites to predict long-term behavior.

To investigate field applications for long-term performance of concrete reinforcement with GFRP bars, flexural tests of beams reinforced with GFRP bars were conducted after exposing those to accelerated and real-time conditionings of up to three-years subjecting to a constant sustained moment (Bakis et al, 2002). Results from this project suggested that changes in bar modulus and strength after conditioning are negligible and bar force at onset of free-end slip is not influenced by the duration or the type of conditioning. Similarly, the study approved by ISIS Canada showed that there was no degradation of the GFRP in the concrete of structures exposed to a wide range of natural environmental conditions for duration of five to eight years (Mufti et al, 2005). On the other hand, a field study showed that the tensile capacity of GFRP bars embedded in concrete slabs for seven years exhibited a significant reduction in some cases more than 20 percent (Treo et al, 2009).

Ductility can be expressed quantitatively as the ratio of the total deformation at failure to the deformation at the elastic limit because conventional steel reinforced beams have a distinct elastic and inelastic phase of deformation before and after yielding of steel. Unlike steel, however, FRP material is brittle in nature with linearly elastic behavior up to failure although it has advantages such as corrosion resistance, high-strength, non-conductivity and light weight. A concept based on deformability rather than ductility has been proposed to ensure that there is sufficient deformation of the structural element RC-GFRP before failure(Jaeger et al.1997). It is adopted to express the concept of ductility by calculating a deformability factor which taking into account moment and curvature at ultimate and service states. It is assumed the value for service stage corresponds to a strain on the GFRP bars of 0.001.

Although these studies are considered to be important in the evaluation of long-term performance of reinforced concrete with GFRP bars, however, it should be noted that few studies have been reported on the long-term performance of reinforced concrete with GFRP bars subjected to simultaneous sustained loading and aging effects of both temperature and humidity in terms of both stiffness/strength degradation and change of deformability after accelerated aging. The purpose of this study was to experimentally investigate the long-term structural degradation of concrete beams with GFRP or steel reinforcement through accelerated conditioning tests.

2. Experimental Programs

2.1 Raw Materials

The concrete mix will utilize Type-A of Portland cement, coarse (19mm) and fine aggregates with 28-day compressive strength of 28MPa. The transverse steel has specified yield strength of 410MPa. Two types of GFRP will be used. One is ASLAN 100 (Type-A, wrapped surface), the other one is VROD HM (Type-B, sand-coated surface, relative high modulus of elasticity). Their mechanical properties of glass fiber reinforced polymer bars, as supplied from the manufacturer, are shown in Table 1.

Table 1 : Mechanical Properties of FRP Bars

FRP Bar Type	Type-A (ASLAN100)		Type-B (V-ROD HM)	
Bar Size	#4	#5	#4	#5
Guaranteed Tensile Strength (MPa)	690	655	1300	1259
Tensile Modulus of Elasticity (GPa)	40.8	40.8	60.0	64.1
Tensile Strain (%)	1.5	1.5	2.42	2.24

2.2 Specimens Fabrication

Dimensions of eighteen specimens, 200mm×300mm×1800mm (Width ×Depth ×Length), will be fabricated. For tensile reinforcement, the longitudinal reinforcement consisted of two-13mm (#4) or three- 16mm (#5) diameters for each specimen. The transverse reinforcement consisted of 10mm (#3) diameter inclined stirrups of steel with the yield strength of 410MPa spaced 120mm and 180mm from the end of the beam. Conventional RC beams with equal dimension and reinforcement ratio of steel will be also fabricated for comparison. The two variables are types of GFRP bars (Type-A and Type-B with relative high modulus of elasticity), types of reinforcement (steel or GFRP), reinforcement area (2-#4/3-#5) and environmental aging (exposure or non-exposure of temperature and humidity up to 300days). The nomenclature of test specimens is as follow; the first character, “GA” or “GH” or “S”, represents the type of reinforcement for glass fiber of type-A , type-B(high MOE) and steel respectively; the second and third characters,”2-3” or “3-5” are the rebar number and size for indicating of reinforcement ratio. For example, 2-4 represents that the reinforcement consists of two-No. 4 bars; the last character varying from 0 to 400 represents the exposure duration (day).

2.3 Sustained Loading for Pre-cracking of Specimens

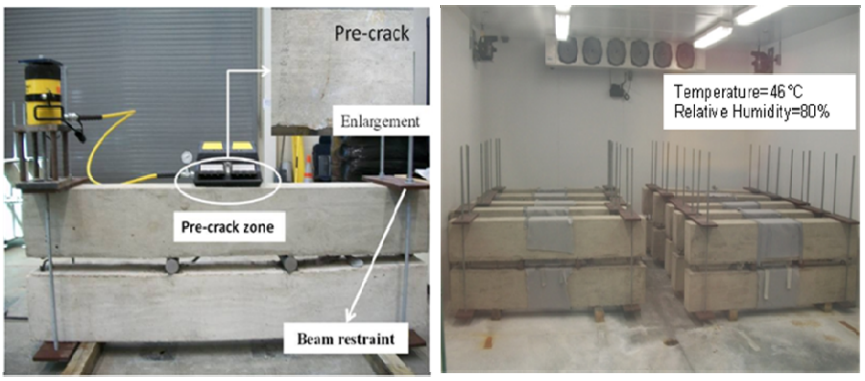

Figure 1 : Pre-jacking for initial crack and exposure in the chamber

All beams will be clamped in pairs using transverse steel rods at the beam end to simulate damages in service conditions as shown in Figure 1. Prior to exposure in the chamber, equal end moments will be applied to the test beams using clamping. The sustained load level will be selected as 0.25P (25% of P) where P is the ultimate flexural load capacity of the beam reinforced with GFRP bars. Constant deformation will be used to prevent release after jacking.

2.4 Accelerated Aging Method in the Chamber

The weather profile in the North-Texas region (DFW area) was considered as the typical exposure profile for the beams. The climate in DFW area is characterized by a hot summer and other humid seasons relatively with moderate seasonal variation in temperature or precipitation through the years. Also, DFW area receives not less than ten sunshine hours per day. For the most aggressive environmental conditions, the test will be focused on choosing average highest temperature of 115°F and average relative humidity of 80% during about last 30 years. For more aggressive environmental condition, the specimens will be exposed to sodium solution consisted of 97% water and 3% sodium chloride. Based on the study by Vijay, the Table 2 shows the correlation between natural exposure in the field and accelerated exposure in the laboratory.

Table 2 : Correlation between Accelerated and Real Exposure by Vijay's Formula*

Temperature of 115°F and RH of 80%		
C (Accelerated exposure in lab.) -days	N (Equivalent-natural exposure) -days	N (Equivalent-natural exposure) -years
100	5999	16.4
200	11998	32.9
300	17997	49.5

Note* : The anticipated natural aging were calculated from Vijay's equation of $N = C \times 0.098e^{0.0558T}$

Where, N=Natural aging (days), C=Chamber aging (days), T=temperature(°F)

2.5 Four Point Bending Test

All specimens will be tested in an MTS machine controlled with Vishay software after conditioning. This machine recorded the load and displacement simultaneously. All tests were displacement-controlled at a rate of 0.2mm/min. Strain gauges will be set up across the center of beams to check the distribution of strain. Comparative studies will be necessary to investigate the various effects by the conditioning. The geometry of beam specimens is also shown in the Figure 2.

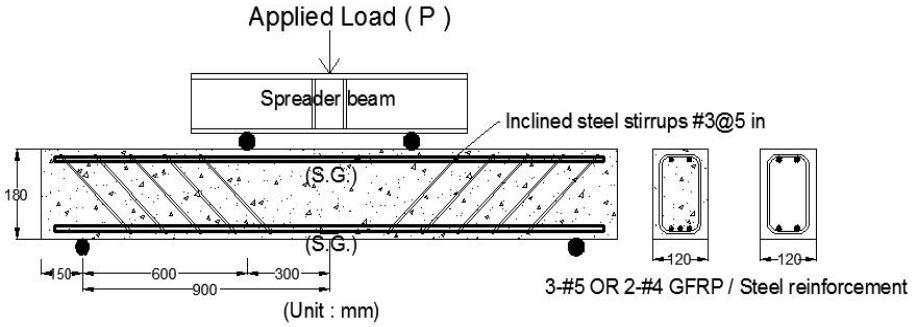

Figure 2 : Details of tested beams

2.6 Loading History

Each testing group is subjected to repeated cycles of loading and unloading until failure was reached, as shown in Figure 3. Energy absorption of GFRP reinforced concrete beams can be obtained in terms of area under the load-deflection curve. To understand the energy absorption in GFRP reinforced concrete sections, load versus deflection of each beam under progressive loading and unloading in seven cycles was noted with each cycle resisting a higher load than the previous cycle as shown in Figure 3. The experimental slopes of unloading curves were recorded.

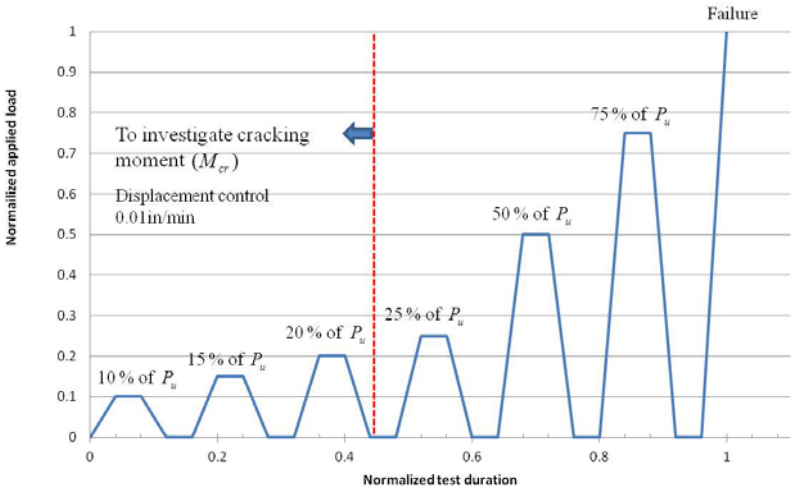

Figure 3 : Loading History

3. Discussion of Test Results

3.1 Mode of Failure and Strain of Rebars

The mode of failure observed for the tested specimens can be divided into three categories. One was balanced failure with simultaneous FRP rupture and concrete crushing in top fiber observed in beams GA2-4-0 and GA2-4-100. Another observed mode was FRP rupture with the under-reinforced section and it was observed in a beam of GA2-4-300. The final mode was local top concrete crushing with the over-reinforced section. The final mode was observed from all specimens except GA2-4 specimens. Table 3 shows the cracking loads, ultimate loads and the deflection corresponding to each loading level. From Table 3, it is obvious that FRP reinforced members (GA and GH-groups) have the least value of $\Delta u/\Delta_{cr}$ and thus are more brittle compared with conventional steel reinforced members(S- group). The increase of duration of accelerated aging could decrease the value of $\Delta u/\Delta_{cr}$ and the decrease is larger in balanced-reinforced members than the over-reinforced-members with the failure mode of concrete crushing.

Figure 4 shows a sample of the measured strain of bottom GFRP and Steel bar. The location of the strain gages were presented in Figure 2. For the beams 2-4 that had the reinforcement consisting of two-No.4 bars, regardless of the type of reinforcement, the bottom bar strains were increased after accelerated aging. In case of GA2-4 beams, the bottom strain at the ultimate stage was 0.022311 recording an increase of 41.9% compared to the specimens not exposed into the environmental chamber for accelerated aging. For the beams of GH2-4 and S2-4, the bottom bar strains at the ultimate state were 0.020109 and 0.029438, respectively. Thus, recording an increase of 41.4% and 20.8% compared to the specimens not exposed into the environmental chamber for accelerated aging respectively.

Table 3 : Experimental bending moments and displacements of specimens at cracking, service and ultimate stages

Specimen I.D	$M_{0.001}$ kN-m	M_{cr} kN-m	M_u kN-m	$\varphi_{0.001}$ μ(1/mm)	φ_u μ(1/mm)	Δ_{cr} mm	Δ_u mm	Failure mode
GA2-4-0	22.1	16.1	63.1	23.7	63.8	1.245	26.746	Balanced
GA2-4-100	22.0	15.7	61.0	24.7	67.2	1.295	27.457	Balanced
GA2-4-300	22.0	15.2	56.6	27.0	75.1	1.372	28.143	FRP-rupture
GA3-5-0	29.7	16.0	84.8	15.5	53.7	0.737	17.551	Concrete crushing
GA3-5-100	29.4	15.9	84.2	16.1	54.5	0.864	18.847	Concrete crushing
GA3-5-300	27.2	15.6	77.8	17.6	58.9	0.991	21.311	Concrete crushing
GH2-4-0	25.5	14.7	72.8	16.4	58.7	1.199	25.476	Concrete crushing
GH2-4-100	24.3	14.4	69.4	18.1	60.5	1.194	25.908	Concrete crushing
GH2-4-300	22.2	14.3	63.6	21.1	67.4	1.092	26.162	Concrete crushing
GH3-5-0	33.0	16.3	100.1	13.4	43.5	0.533	15.773	Concrete crushing
GH3-5-100	32.0	15.8	96.9	14.6	46.5	0.686	16.993	Concrete crushing
GH3-5-300	27.8	15.7	84.4	16.5	48.3	0.787	20.752	Concrete crushing
S2-4-0	31.2	15.0	49.4	10.4	79.4	0.787	31.013	Concrete crushing
S2-4-100	30.3	14.8	47.9	11.0	87.0	0.635	33.553	Concrete crushing
S2-4-300	28.7	12.0	39.3	11.6	95.9	0.533	40.945	Concrete crushing
S3-5-0	34.0	15.1	74.4	8.0	70.6	1.143	17.452	Concrete crushing
S3-5-100	33.9	15.0	73.0	8.2	74.6	0.838	17.577	Concrete crushing
S3-5-300	32.6	12.0	67.3	9.4	82.6	0.787	29.083	Concrete crushing

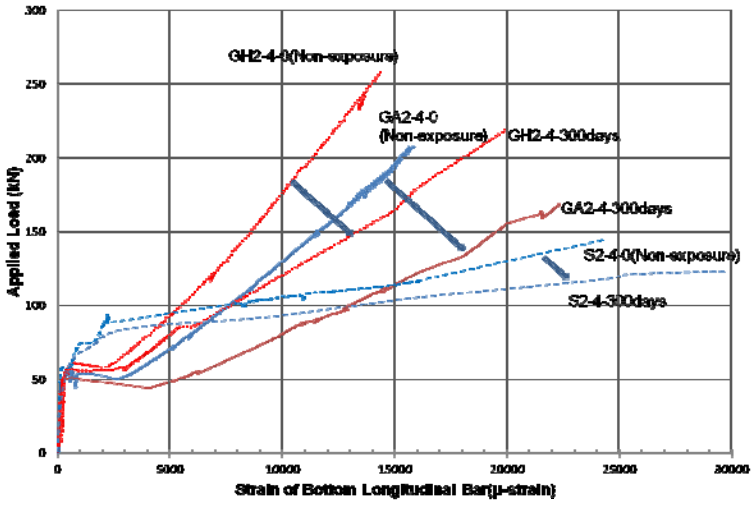

Figure 4 : Load-Strain Relationship of Bottom Bar of Beams

3.2 Load Deflection Behavior

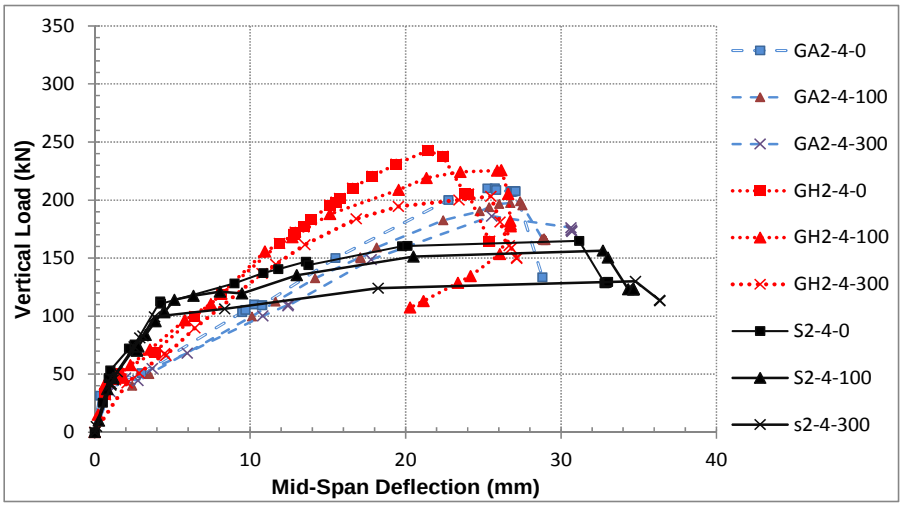

Figure 5 : Load-vertical deflection of the tested beams(2-#4 of Each Case)

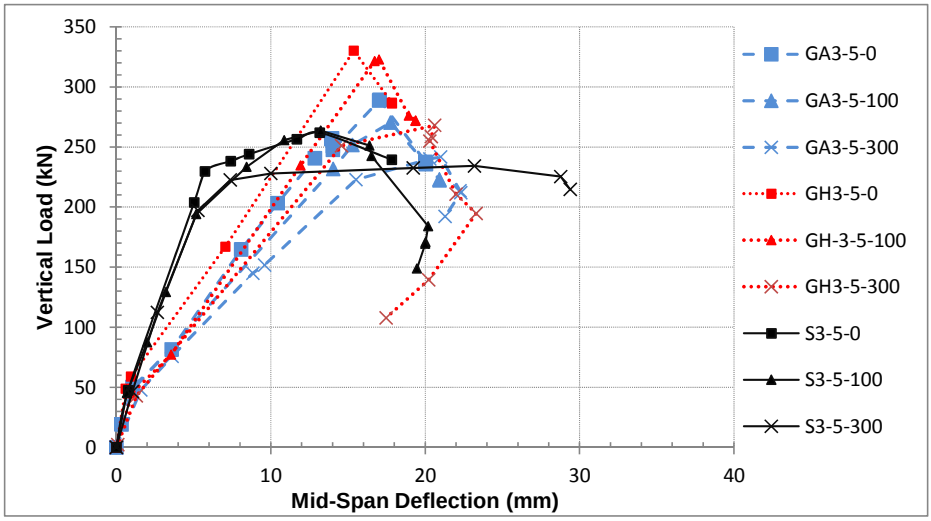

Figure 6 : Load-vertical deflection of the tested beams(3-#5 of Each Case)

Figure 5 and 6 show the total applied load and vertical deflection curves for all the tested specimens. For GA2-4 and GA3-5 with Type-A of reinforcement, the first observed cracks were at moments equal to 16kN-m. These measured cracking moments were about 25.5% and 18.9% of ultimate loads of beams GA2-4-0 and GA3-5-0, respectively. For GH2-4 and GH3-5 with Type-B of reinforcement, the first observed cracks were at moments equal to 12 and 16kN-m, respectively. These measured cracking moments were about 17.9% and 16.3% of ultimate loads of beams GH2-4-0 and GH3-5-0, respectively. For S2-4 and S3-5 with steel reinforcement, the first observed cracks were at moments equal to 15kN-m, respectively. These measured cracking moments were about 30.4% and 20.5% of ultimate loads of beams S2-4-0 and S3-5-0, respectively. It is noted that no significant changes were observed between the unexposed RC-GFRP/Steel beams and ones placed in the chamber up to 300days for environmental exposure.

In all cases, however, the moment carrying capacity decreased and the deflection increased as a function of time when exposed to accelerated aging. GA2-4, GH2-4 and S2-4 exhibited the reduction of load-carrying capacity of approximately 12%, 13% and 21%, respectively, after 300days in environmental chamber while the increase of deflection were 5.2%,2.7% and 25.5%. GA3-5, GH3-5 and S3-5 exhibited the reduction of load-carrying capacity of approximately 8.3%, 11.2% and 12.5%, respectively, after 300days in environmental chamber while the increase of deflection were 21.4%,31.4% and 66.1% respectively. The figures indicate that under the aggressive conditions in which the specimens were exposed, significant loss of load-carrying capacity could occur. It should be noted, however, not only that the change of load-carrying capacity in RC-steel specimens is greater than the one in RC-GFRP specimens but also that beams exposed into the environmental chamber show relatively gradual member compression failures compared with the more brittle failures of the non-exposed specimens.

3.3 Change of deformability

The moment-deformation based model (the Jaeger index) was introduced by Jaeger et al. taking into account the strength effect of moment as well as the curvature (or deflection) effect on the ductility. For the deformability of the Jaeger index (equation 1), margin between the service stage and the ultimate stage reflect the ductility. Moment and curvature at ultimate state are used as well as the moment and curvature at service state. The service limit stage corresponds to the value at concrete compressive strain of 0.001 considered as the beginning of inelastic deformation of concrete top compression fiber.

$$[1]\quad \mu_E = \left(\frac{\varphi_u}{\varphi_{0.001}}\right) \times \left(\frac{M_u}{M_{0.001}}\right)$$

Where M_u and φ_u are the moment and curvature at ultimate stage; $M_{0.001}$ and $\varphi_{0.001}$ are the moment and curvature at service stage respectively.

Table 4 shows the value of deformability factor (DF). Comparison of DF for compression failures of RC-GFRP beams and RC-steel beams indicates that the values are not similar. In terms of the type of reinforcement, RC-Steel specimens exhibited the increase of DF as the increase of exposure duration unlike RC-GFRP ones. A steel reinforced beam with a compression failure was found to have a DF of 10.2(Park and Paulay,1975) using energy-based DF model. The values of DF in deformation-based method of Jaeger index are not similar to ones by energy-based method.

Table 4: Change of Deformability Factor

Specimen I.D	Deformability factor (D.F.)	Normalized D.F.	Specimen I.D	Deformability factor (D.F.)	Normalized D.F.
GA2-4-0	7.69	1.00	GA3-5-0	9.88	1.00
GA2-4-100	7.52	0.98	GA3-5-100	9.67	0.98
GA2-4-300	7.14	0.93	GA3-5-300	9.55	0.97
GH2-4-0	10.22	1.00	GH3-5-0	11.82	1.00
GH2-4-100	9.53	0.93	GH3-5-100	11.65	0.98
GH2-4-300	9.14	0.89	GH3-5-300	10.90	0.92
S2-4-0	12.05	1.00	S3-5-0	19.29	1.00
S2-4-100	12.49	1.04	S3-5-100	19.50	1.01
S2-4-300	12.82	1.06	S3-5-300	19.69	1.02

Although there are differences between ways to calculate the ductility index, it can be seen that the Jaeger index shows the consistent tendency by time-dependent environmental exposure regardless of the ratio of reinforcement. Moreover, in the Jaeger index, the deformability factors were much higher than the minimum value of four as proposed in ISIS Canada design manual No.3 for RC members reinforced with FRP of the minimum requirement. The changes of DFs of the sections with type-B reinforcement (with sand-coated surface) were greater than ones with type-A of reinforcement (with wrapped surface)

4. Conclusion and Future Work

Test results on 18-GFRP and steel reinforced concrete beams are presented in this paper. Three different reinforcements, different reinforcement amounts and different exposure duration were used. This paper focuses the flexural performances of specimens as well as the deformability evaluation after accelerated aging. From the results of this study, the following conclusions can be made:

- In all cases, the moment carrying capacity decreased and the deflection increased as a function of time when exposing in circumstances for accelerated aging.
- The change of load-carrying capacity in RC-steel specimens is greater than the one in RC-GFRP specimens.
- Beams exposed in the environmental chamber showed a tendency to be less brittle in the mode of failure as compared to those not exposed
- For type-A, type-B and steel reinforcement, DFs were observed in the range 7.14 to 9.55, 9.14 to 11.82 and 12.05 to 19.69.
- The deformability factors of RC-GFRP showed a tendency to be decreased after accelerated aging while DFs of RC-steel increased after accelerated aging.

As a complement to the tests for flexural performances, data of direct tensile test of rebars are currently under investigation in order to make a correlation model of accelerated and real-time conditioning. This model will verify the relationship between real time-degradation and accelerated degradation. Moreover, evaluation of stiffness degradation will be performed according to the change of effective moment of inertia. RC-GFRP or steel should be designed with enough deformability. Since so far there is no general agreement on how much deformability is enough, further study is necessary to evaluation of the deformability after accelerated aging by using several ways to calculate the deformability indices,

Determination of long term performance is a recognized but less-mentioned topic in the sector of the reinforced concrete with FRP bars to improve moment capacity by its high tensile strength. The information in these areas is still unclear or in need of additional evidence to validate long-term performance. With the following additional future works adding these 18 tested beams, better information of long-term structural performances of concrete beams with GFRP or steel reinforcement through short-term accelerated conditioning tests will be obtained.

Acknowledgments

The work described in this paper has been supported by Hughes Brothers Inc. and Concrete Protection Product. Inc.

References

ACI-440.1R-06, 2006, Guide for the Design and Construction of Structural Concrete Reinforced with FRP Bars

ASCE, 2009,Report card for america's infrastructure, 75-76

Bank,L.C, Gentry, T.R., Barkatt, A., 1995, Accelerated test methods to determine the long-term behavior of FRP composite structures-environmental effects,Journal of reinforced plastics and composites , v14, 559-587

Benmokrane, B. and Chaallal, O.,1996, Flexural response of concrete beams reinforced with FRP reinforcing bars, ACI structural journal , 93(1) ,46-55

Helbling, C.S., Karbhari, V.M., 2002, Environmental durability of E-glass composites under the combined effect of moisture, temperature and stress: CDCC'02,247-258

ISIS Canada research network, 2007, Reinforcing Concrete Structures with Fibre Reinforced Polymers, Design manual No.3, 2nd ed.

Jaeger LG, Mufti AA,Tadros, G.,1999,The concept of the overall performance factor in rectangular-section reinforced concrete members. In: Proc of 3rd int. Symp. on non-metallic (FRP) reinforcement for concrete structures.,v2, 551-559.

Litherland, K.L., Oakley, D.R., Proctor, B.A.,1981, The use of accelerated ageing procedure to predict the long term strength of GRC composite: Cement and concrete research : v11,455-466

Mufti, M., Benmokrane,B, Banthia,N, Newhook,J,: Durability of GFRP reinforced concrete in field structures ,7th-FRPRCS, SP-230-77 , 1361-1377

Naaman AE, Jeong SM.,1995, Structural ductility of concrete beams pre-stressed with FRP tendons. In Proceedings, 2nd int. RILEM Symp. FRPRXS-2. Non-metric (FRP) Reinforcement for concrete structures. RILEM, 379-386.

Toutanji HA, Saafi M.,2000, Flexural behavior of concrete beams reinforced with glass fiber-reinforced polymer (GFRP) bars. ACI Struct J.,v97(5),712–719.

Trejo, D., Gardoni, P., Kim, J,2009, Long term performance of GFRP reinforcement , Technical report (TxDot)-0-6069

Vijay, P.V., GangaRao, H.V., 1999, Accelerated and natural weathering of glass fiber reinforced plastic bars, 4th international conference on FRPRCS, 605-614